Vol. 15 (núm 1) pp. 121 - 129
Enero - Junio 2024
https://doi.org/10.19053/01217488.v15.n1.2024.15857

Control Evaluation for a Boost Converter via the PI-PBC & IOC-PI Theories for Voltage Support in Linear Loads: Numerical validations in PSIM, PLECS, and MATLAB/Simulink

Evaluación de controladores para un convertidor elevador mediante las teorías PI-PBC & IOC-PI para soporte de tensión en cargas lineales: validaciones numéricas en PSIM, PLECS y MATLAB/Simulink

J. S. Gómez-Chitiva[1], A. F. Escalante-Sarrias, Oscar Danilo Montoya[1]

Abstract

This paper presents a comparison of the voltage and current dynamic responses for the Boost converter in three different simulation software, namely PSIM, PLECS, and MATLAB/Simulink, while using two types of nonlinear controllers. The utilized controller designs are (i) proportional-integral passivity-based control (PI-PBC) and (ii) inverse optimal control with PI action (IOC-PI). The main advantage of the PI-PBC and IOC-PI controllers is that both ensure the stable operation of the converter via Lyapunov's stability theory. In addition, in both controllers, integral action enables the elimination of non-modeled dynamics in the converter by allowing it to reach the reference with minimal stabilization times. The results showed that, despite the fact that all utilized simulation software applications had their advantages, the one with the best dynamic response for both nonlinear controls was PSIM. Moreover, it is easier to use for someone who has never worked with a simulation environment. The main objective of this research was to compare simulation software and find the most suitable environment for evaluating and implementing nonlinear control with regard to power electronic converter applications.

Keywords: PSIM, MATLAB/Simulink, PLECS, Boost converter, nonlinear control, PI-PBC, IOC-PI

Resumen

Este artículo presenta una comparación de las respuestas dinámicas de voltaje y corriente en el convertidor Boost en tres *software* de simulación diferentes, a saber: PSIM, PLECS y MATLAB/Simulink, utilizando dos tipos de controladores no lineales. Los diseños de controlador utilizados son (i) el control basado en pasividad integral proporcional (PI-PBC) y (ii) el control óptimo inverso con acción PI (IOC-PI). La principal ventaja de los controladores PI-PBC e IOC-PI es que ambos aseguran el funcionamiento estable del convertidor a través de la teoría de estabilidad de Lyapunov. Además, en ambos controladores, la acción integral permite eliminar dinámicas no modeladas en el convertidor al permitirle alcanzar la referencia con tiempos mínimos de estabilización. Los resultados mostraron que, a pesar de que todos los *software* de simulación que se utilizaron tenían sus ventajas, el que presentó una mejor respuesta dinámica para ambos controles no lineales fue PSIM. Además, es más sencillo de utilizar para alguien que nunca haya trabajado con un entorno de simulación. El objetivo principal de esta investigación fue comparar algunos *software* de simulación y encontrar el entorno más adecuado para la evaluación e implementación del control no lineal en aplicaciones de convertidores electrónicos de potencia.

Palabras Clave: PSIM, MATLAB/Simulink, PLECS, Convertidor elevador, Control no lineal, PI-PBC, IOC-PI

Recepción: 04-Abril-2023
Aceptación: 06-Agosto-2023

[1]Grupo de Compatibilidad e Interferencia Electromagnética (GCEM), Facultad de Ingeniería, Universidad Distrital Francisco José de Caldas, Bogotá 110231, Colombia.
[1,*] Grupo de Compatibilidad e Interferencia Electromagnética (GCEM), Facultad de Ingeniería, Universidad Distrital Francisco José de Caldas, Bogotá 110231, Colombia. Dirección electrónica: odmontoyag@udistrital.edu.co

1 Introduction

The continuous development of technology around the world has caused the energy demand to increase exponentially, thus making it a predominant factor [1]. This is why the electric infrastructure has been strengthened with the addition of renewable energy sources, among other things [2]. This addition brings with it the use of converters, inverters, and other power electronic circuits, aiming to regulate the output voltage in the face of load or/and input voltage variations [3].

The addition of new technologies such as photovoltaic (PV) generators and/or wind farms which incorporate said power electronic circuits can aid in the process of supplying energy through high-voltage direct current transmission (HVDC) to electric systems, which has more benefits than high-voltage alternating current transmission (HVAC) in the form of lower power losses and the avoidance of reactive power, among others [4]. The use of new control techniques that maximize the performance of converters in order to minimize power losses is an important task to consider regarding the future development of power systems. Therefore, the development of nonlinear control techniques is important in power systems, as most of their subsystems are not linear.

The most common DC-DC converter types are Buck, Boost, and Buck-Boost, which can be seen in industrial applications such as DC-regulated energy sources, DC motor speed braking, battery charging, and UPS, among others [5]–[7]. Control in DC-DC converters has been widely studied with the purpose of finding the best dynamic response, and some control techniques, linear or not, can be found in the literature, such as PID control [8], sliding mode control [9], voltage mode control [10], PI passivity-based control [11], and inverse optimal control with PI action [12], among others.

To understand how converters work in different applications, the specialized literature commonly uses simulation software in order to predict their dynamics in open- or closed-loop control, before implementing them in real scenarios. Some common simulation software applications for power electronics which can be found in the industry are PSIM [13], PLECS [14], MATLAB/Simulink [15], and LTSpice XVII [16], among others. Despite the fact that there are papers that present simulation results obtained from different types of simulation software for multiple power electronics applications [17], [18], the state of the art has not addressed the nonlinear control applications of DC-DC converters. Thereupon, this paper is an opportunity to contribute to power electronics research by describing the advantages and disadvantages of multiple simulation software applications (PSIM, PLECS, and MATLAB/Simulink) in nonlinear control techniques (PI-PBC and IOC-PI controllers) for power electronic circuits.

The structure of this paper is as follows: Section 2 shows the general definition and structure of Boost converters; Section 3 summarizes the nonlinear control techniques implemented in this research; Section 4 presents the numerical validation in PSIM, PLECS, and MATLAB/Simulink, showing the voltage and current dynamic response of the Boost converter in a closed-loop via PI-PBC and IOC-PI control; and Section 5 presents the main conclusions of this research.

2 General structure of a Boost converter

Also known as a *step-up* (see Fig. 1), the output voltage of a Boost converter is higher than the input voltage. Its main application involves DC-regulated energy sources and DC motor regenerative speed braking [5].

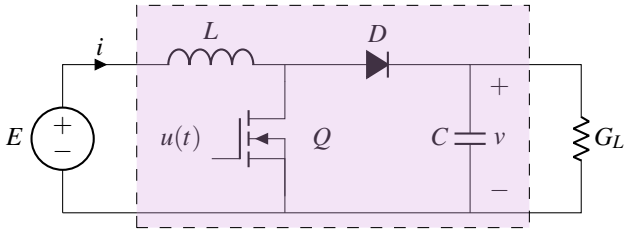

Figure 1: Boost converter

The variables and parameters in Fig. 1 can be interpreted as follows: $E > 0$ corresponds to the input voltage in volts (V); $i > 0$ (also known as x_1) represents the associated current of the inductor L in amperes (A); v (also known as x_2) represents the output voltage associated with capacitor C in V; G_L is the variable load in siemens ($\mho$); and $u \; \varepsilon \; [0-1]$ represents the input control variable applied for the forced commutation of the transistor (dimensionless quantity).

3 Dynamic model and controller designs

This section presents the general dynamic modeling of the Boost converter using the averaging theory [19]. The PI-PBC and IOC-PI designs will be developed based on this mathematical model. To obtain the mathematical model of the Boost converter, Kirchhoff's second law is applied to the closed-loop trajectory, which includes the capacitor, voltage source, and diode, thus yielding Equation (1).

$$L\dot{x}_1 = (1-u)\,x_2 + E. \tag{1}$$

Now, to obtain the dynamic behavior of the voltage through the capacitor, Kirchhoff's first law is applied to the node where the capacitor, the resistive load, and the diode are connected, which leads to Equation (2).

$$C\dot{x}_1 = -(1-u)\,x_1 - G_L x_2. \tag{2}$$

Remark 1 *The average dynamic model of the boost converter in Equations (1) and (2) can be represented as a general port-Hamiltonian system whose structure is shown in (3) [20].*

$$\mathscr{D}\dot{x} = (\mathscr{J}_0 + \mathscr{J}_1(u) - \mathscr{R})\,x + \zeta, \tag{3}$$

where $\mathscr{D}$ is a positive definite matrix regarding the energy storage devices, i.e., the inductors and the capacitor; $\mathscr{J}_0$ and $\mathscr{J}_1(u)$ are skew-symmetry matrices known as the interconnection matrices; $\mathscr{R}$ is a positive semi-definite matrix associated with damping effects on the dynamic model; ζ is a vector of external inputs; and x is the vector containing the state variables. These elements are presented below.

$$\mathscr{D} = \begin{bmatrix} L & 0 \\ 0 & C \end{bmatrix}, \ \mathscr{J}_0 = \begin{bmatrix} 0 & 1 \\ -1 & 0 \end{bmatrix}, \ x = \begin{bmatrix} x_1 \\ x_2 \end{bmatrix},$$
$$\mathscr{J}_1(u) = \begin{bmatrix} 0 & -u \\ u & 0 \end{bmatrix}, \ \mathscr{R} = \begin{bmatrix} 0 & 0 \\ 0 & G_L \end{bmatrix}, \ \zeta = \begin{bmatrix} E \\ 0 \end{bmatrix}.$$

To obtain a general control design for the Boost converter in Figure 1 while considering the average dynamic modeling in Equation (3), the dynamic model at the equilibrium point must be defined [11]. In general, if $x_1^\star$, $x_2^\star$, and $u^\star$ are defined as the operating points for the state variables and the control input, then (3) takes the form of (4) under steady-state conditions.

$$\mathscr{D}\dot{x}^\star = (\mathscr{J}_0 + \mathscr{J}_1(u^\star) - \mathscr{R})x^\star + \zeta. \tag{4}$$

Note that, if the error variables $\tilde{x}_1$, $\tilde{x}_2$, and $\tilde{u}$ are defined as $x_1 - x_1^\star$, $x_2 - x_2^\star$, and $u - u^\star$, respectively, and if (3) and (4) are combined, then the general dynamics of the error model are reached, as presented in (5).

$$\mathscr{D}\dot{\tilde{x}} = (\mathscr{J}_0 + \mathscr{J}_1(u) - \mathscr{R})\tilde{x} + \mathscr{J}_1(\tilde{u})x^\star. \tag{5}$$

Remark 2 *By considering the properties of the skew-symmetry matrix $\mathscr{J}_1(\tilde{u})$ multiplied by the vector of the state variables at the desired operating point (i.e., $x^\star$), the dynamics of the error model (5) can be rewritten as follows, using an auxiliary vector $g(x^\star)$.*

$$\mathscr{D}\dot{\tilde{x}} = (\mathscr{J}_0 + \mathscr{J}_1(u) - \mathscr{R})\tilde{x} + g(x^\star)\tilde{u}, \tag{6}$$

where the controller design focuses on finding $\tilde{u}$, such that $\lim_{t\to\infty}\tilde{x} \to 0$, i.e., on finding a control input that ensures asymptotic convergence [21]. It is worth mentioning that

$$\mathscr{J}_1(\tilde{u})x^\star = \begin{bmatrix} 0 & -u^\star \\ u^\star & 0 \end{bmatrix}\begin{bmatrix} x_1^\star \\ x_2^\star \end{bmatrix} = \begin{bmatrix} -x_2^\star \\ x_1^\star \end{bmatrix}\tilde{u} = g(x^\star)\tilde{u}.$$

3.1 PI passivity-based control (PI-PBC)

Passivity-based control theory is a strong, mathematically founded control theory that is applicable to a subclass of dynamical systems which have a port-Hamiltonian structure [22], with the main advantages that (i) the open-loop port-Hamiltonian structure is preserved in closed-loop design, *i.e.*, the passivity properties of the model are maintained [23], [24]; and (ii) a stable closed-loop operation can be ensured via Lyapunov's stability theory [25].

In the case of port-Hamiltonian models with a strictly bilinear structure and without any additional nonlinearity, the most suitable control based on this theory corresponds to PI-PBC design [26]. This type of controller has the main advantage that it ensures asymptotic convergence and includes a set of integral actions that allow minimizing the steady-state errors introduced by unmodeled dynamics [27].

Remark 3 *The general control law for PI-PBC design in a power electronic converter with a strictly bilinear structure, as defined in (3), is shown in (7) and (8).*

$$u = \widetilde{u} + u^\star = -k_p\widetilde{y} + k_i z + u^\star, \tag{7}$$
$$\dot{z} = -\widetilde{y}, \tag{8}$$

where $\tilde{u}$ is equal to $-k_p\widetilde{y} + k_i z$, with k_p and k_i being two positive definite constants associated with the proportional and integral gains. Note that $\tilde{y}$ for port-Hamiltonian systems is known as the passive output [11].

3.1.1 Calculating the equilibrium point

To determine the values of $u^\star$ and $x_1^\star$ which allow supporting the voltage profile at the terminals of the constant resistive load (*i.e.*, the $x_2^\star$), Equation (4) is solved by assuming that $\dot{x}^\star$ is zero due to the fact that, for the boost converter, the desired operating point is constant. The above yields (9).

$$\begin{aligned} \mathscr{J}_1(u^\star)x^\star &= -(\mathscr{J}_0 - \mathscr{R})x^\star - \zeta, \\ g(x^\star)u^\star &= -(\mathscr{J}_0 - \mathscr{R})x^\star - \zeta. \end{aligned} \tag{9}$$

Note that solving (9) to find the controller structure at the equilibrium point (*i.e.*, $u^\star$) requires multiplying $g(x^\star)$ by the transposed vector, *i.e.*, $g^\top(x^\star)$, which produces

$$\begin{aligned} g^\top(x^\star)g(x^\star)u^\star &= -g^\top(x^\star)((\mathscr{J}_0 - \mathscr{R})x^\star + \zeta), \\ u^\star &= -\mathscr{G}(x^\star)\left(g^\top(x^\star)((\mathscr{J}_0 - \mathscr{R})x^\star + \zeta)\right), \end{aligned} \tag{10}$$

where $\mathscr{G}(x^\star) = \left(g^\top(x^\star)g(x^\star)\right)^{-1}$.

Note that the solution of Equation (10) for the boost converter model in (3) is the following:

$$u^* = 1 - \frac{E + G_L x_1^*}{x_2^{*2} + x_1^{*2}}x_2^*. \tag{11}$$

On the other hand, to obtain the reference value for the current variable through the inductor (*i.e.*, $x_1^\star$), the left-annihilator of $g()$ is used, which is formulated as follows:

$$h(x^\star) = \begin{bmatrix} x_1^\star \\ -x_2^\star \end{bmatrix},$$

which, when pre-multiplied from the left to right with (9), generates the following equation:

$$h^\top(x^\star)g(x^\star)u^\star = -h^\top(x^\star)((\mathscr{J}_0 - \mathscr{R})x^\star + \zeta) = 0. \tag{12}$$

The solution of Equation (12) for the Boost converter model in (3) is the following:

$$x_1^* = \frac{G_L x_2^{*2}}{E}. \tag{13}$$

3.1.2 Stability analysis

The main advantage of using passivity-based control theory is that the control law in (7) and (8) preserves the passivity properties in closed-loop operation [28]. In addition, part of the candidate Lyapunov function is constructed by using the Hamiltonian function of the system, *i.e.*, the energy storage function of the dynamic system. For the Boost converter, the Hamiltonian function ($H(\tilde{x})$) takes the following form:

$$H(\tilde{x}) = \frac{1}{2}\left(L\tilde{x}_2^2 + C\tilde{x}_2^2\right) = \frac{1}{2}\tilde{x}^\top \mathscr{D}\tilde{x}. \tag{14}$$

Note that the main characteristic of the Hamiltonian function in (14) is that it is a positive definite function that is zero only when the error variables have reached their operating point.

Now, to verify whether the PI-PBC design in (7) and (8) ensures stability during closed-loop operation in the sense of Lyapunov, let us define a candidate Lyapunov functions with the structure presented in (15).

$$V(\tilde{x}, z) = H(\tilde{x}) + \frac{1}{2}z^\top k_i z, \tag{15}$$

where a positive definite function is observed which fulfills the first Lyapunov stability condition, *i.e.*, $V(\tilde{x}, z)$ is zero if and only if $(\tilde{x}, z) = (0, 0)$. Now, to determine whether the time derivative of the candidate Lyapunov function $V(\tilde{x}, z)$ is negative definite or semi-definite, Equation (15) is differentiated with respect to time.

$$\begin{aligned} \dot{V}(\tilde{x}, z) &= \dot{H}(\tilde{x}) + \frac{1}{2}z^\top k_i \dot{z}, \\ \dot{V}(\tilde{x}, z) &= \tilde{x}^\top \mathscr{D}\dot{\tilde{x}} + \frac{1}{2}z^\top k_i \dot{z}. \end{aligned} \tag{16}$$

If Equation (16) is substituted into (5), (7), and (8), the following is obtained:

$$\dot{V}(\tilde{x}, z) = \begin{bmatrix} \tilde{x}^\top \left(\left(\mathscr{J}_0 + \mathscr{J}_1(u) - \mathscr{R} \right) \tilde{x} \right) \\ \tilde{x}^\top g(x^\star)\tilde{u} + z^\top k_i(-\tilde{y}) \end{bmatrix}. \tag{17}$$

In (17), considering the properties of the skew-symmetry matrices $\mathscr{J}_0$ and $\mathscr{J}_1(u)$, it is observed that $\left(\tilde{x}^\top \mathscr{J}_0 \tilde{x}\right) = 0$, and $\left(\tilde{x}^\top \mathscr{J}_1(u)\tilde{x}\right) = 0$. In addition, note that $\tilde{y}^\top = \tilde{x}^\top g(x^\star)$, which implies that:

$$\begin{aligned} \dot{V}(\tilde{x}, z) &= -\tilde{x}^\top \mathscr{R}\tilde{x} + \tilde{x}^\top g(x^\star)\tilde{u} - z^\top k_i \tilde{y}, \\ &= -\tilde{x}^\top \mathscr{R}\tilde{x} + \tilde{y}^\top(-k_p\tilde{y} + k_i z) - z^\top k_i \tilde{y}, \\ &= -\tilde{x}^\top \mathscr{R}\tilde{x} - \tilde{y}^\top k_p \tilde{y} \leq 0, \end{aligned} \tag{18}$$

where it is observed that $\dot{V}(\tilde{x}, z)$ is lower than or equal to zero, *i.e.*, the PI-PBC controller in (7) and (8) ensures closed-loop stability in the sense of Lyapunov for the dynamics of the error model in (6). For additional details regarding the application of PI-PBC theory to DC-DC converters, see [11] and [29].

3.2 Inverse optimal control with PI action (IOC-PI)

Inverse optimal control theory is a sub-field of optimal control design that exploits some characteristics of nonlinear systems in order to obtain a general controller by selecting a general control output that will minimize some functional [30]; the main advantage of IOC is that, for power electronic converters a with bilinear structure, the applicable control input is well known and ensures asymptotic stability in the sense of Lyapunov [12], with the possibility of adding an integral gain without affecting stability properties during closed-loop operation.

The general IOC-PI control law for a Boost converter feeding a linear load is presented in Equations (19) to (21).

$$u = u^\star + \tilde{u}, \tag{19}$$

$$u^\star = 1 - \frac{E}{x_2^\star}, \tag{20}$$

$$\tilde{u} = \frac{1}{2}\left(k_p\left(x_2^\star \tilde{x}_1 - x_1^\star \tilde{x}_2\right) + k_i \int \left(x_2^\star \tilde{x}_1 - x_1^\star \tilde{x}_2\right) dt\right), \tag{21}$$

where $u^\star$ is reached after solving the first row of (6), and $x_1^\star$ is the reference presented in (14).

Remark 4 *The main characteristic of the control input to regulate the error, i.e., $\tilde{u}$ in (2), is that it can be represented as a function of the passive output $\tilde{y}$ as follows:*

$$\begin{aligned} \tilde{y} &= \left(\tilde{x}^\top g(x^\star)\right)^\top = g^\top(x^\star)\tilde{x}, \\ \tilde{y} &= x_1^\star \tilde{x}_2 - x_2^\star \tilde{x}_1, \end{aligned} \tag{22}$$

which implies that (20) can be represented using (22):

$$\tilde{u} = -\frac{1}{2}\left(k_p\tilde{y} + k_i \int \tilde{y} dt\right). \tag{23}$$

Note that, in order to demonstrate closed-loop stability for the IOC-PI controller, the following candidate Lyapunov function can be used:

$$V(\tilde{x}, z) = H(\tilde{x}) + \frac{1}{4}z^\top k_i z. \tag{24}$$

The reader could review [12] for further information on IOC-PI theory for DC-DC converters.

4 Numerical validations

The design of PI-PBC and IOC-PI controllers for the Boost converter was validated through PSIM, PLECS, and MATLAB/Simulink while considering the parameters shown in Table 1 [11].

During all numerical validations, the following facts were considered to demonstrate the effectiveness and strength of each simulation software:

Table 1: Boost converter parameters for the studied case

Parameter	Symbol	Value	Unit
Input voltage	E	12	V
Inductance	L	25	μH
Capacitance	C	31	μF
Conductance 1	G_{L_1}	1/8	℧
Conductance 2	G_{L_2}	1/4	℧
Reference voltage	x_2^*	24	V
Reference controller	u^*	50	%

i. The initial voltage of the capacitor was equal to the reference voltage x_2^* in Table 2. Due to convergence problems in all simulation applications, the initial current in the inductor was set at 0 A at the beginning of the simulation.

ii. The system was initially positioned with the load G_{L2}. The software had two loads with the same value G_{L1} in parallel. After 2.5 ms, the load changed, leaving a single load equal to G_{L1}. This process was repeated twice, for a total time of 10 ms.

All simulations were run in a desktop computer with an Intel(R) Core(TM) i5-4210U CPU @ 1.70-2.40 GHz, 8.00 GB of installed RAM, and a 500 GB SATA SSD, running a 64-bit version of windows 10 Home.

The specific software applications used for the validation of each nonlinear control were PSIM version 2022.2.0.17, PLECS version 4.1.2, and MATLAB/Simulink version R2021b.

The general implementation of the electronic circuit related to the Boost converter in each simulation software is depicted in Figures 2, 3, and 4. Note that the electronic circuit of each simulator generally has the same constituting elements.

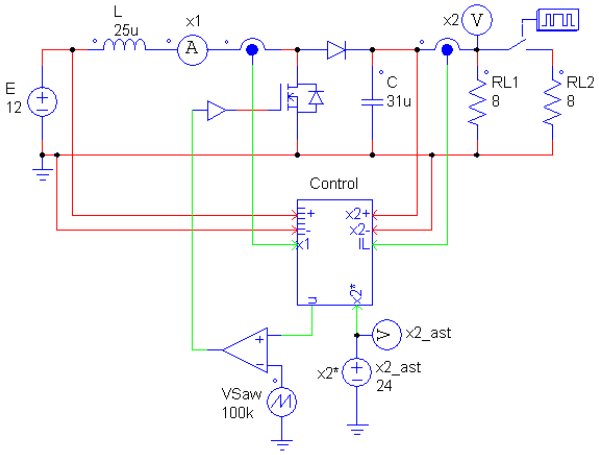

Figure 2: Implementation of the Boost converter in the PSIM software

The variable load was used when implementing the equations (the general linear load corresponds to the G_L parameter), so obtaining that value from the circuit required some

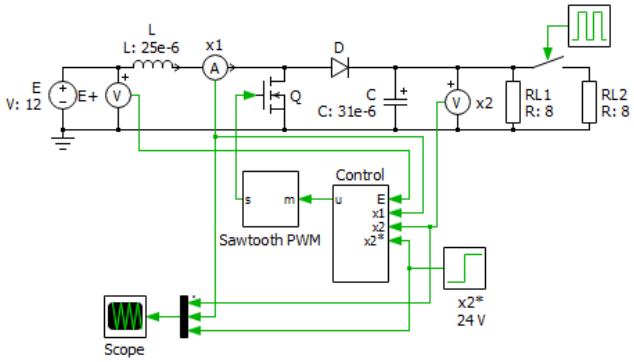

Figure 3: Implementation of the Boost converter in the PLECS software

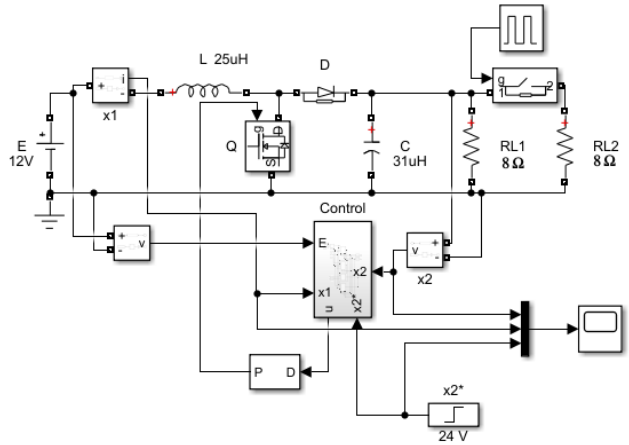

Figure 4: Implementation of the Boost converter in the MATLAB/Simulink software

algebraic calculations. In PSIM, this value can be obtained from the circuit while using sensors and Ohm's law. In PLECS and MATLAB/Simulink, it is not possible to obtain said value from the circuit itself due to a simulation convergence error. For each simulation software, the implementation of load variations is presented in Figures 5, 6, and 7.

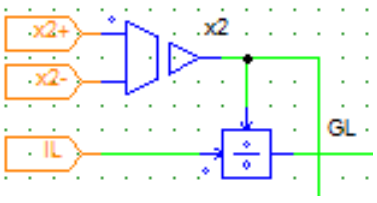

Figure 5: Implementation of the load variations in the PSIM software

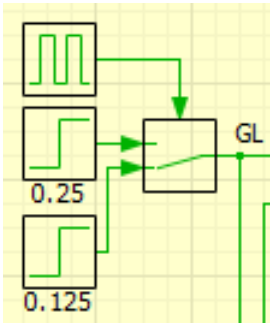

Figure 6: Implementation of the load variations in the PLECS software

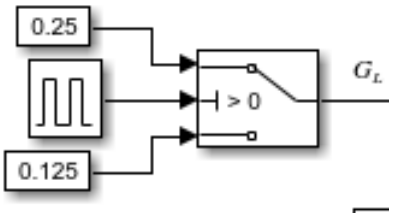

Figure 7: Implementation of the load variations in the MATLAB/Simulink software

During the numerical simulations, it is important to mention that:

i. The output voltage x_2 is the red signal (V).

ii. The reference output voltage x_2^* is the black signal (V).

iii. The current flowing through the inductor x_1 is the blue signal (A).

iv. The reference current through the inductor x_1^* is the green signal (A).

The PSIM software performs the validation in 0-100 ms. The reason for selecting that period is that the signal must stabilize in this software, and this interval is enough for that. The signals bounded in purple represent the dynamic response between 0 ms and 10 ms, and the ones bounded in cyan represent the dynamic response between 90 ms and 100 ms. In PLECS and MATLAB/Simulink, the validation is carried out between 0 ms and 10 ms because it is unnecessary to wait for stabilization; the behavior is the same at any given moment.

4.1 PI-PBC validation

According to Remark 3, the general control law for this theory uses two positive proportional constants, namely k_p and k_i, which, for the sake of validation, are 0.0099 and 0.0009, respectively, and are taken from [11].

Figure 8 shows the dynamic response of the Boost converter when the PI-PBC controller is implemented in PSIM. In this case, the signal does not reach the reference at the beginning, so the simulation period is extended when compared to the other software applications. Despite the long period necessary to obtain the correct dynamic response, PSIM does not take too long to simulate it. In the signal, in the section bounded in cyan (Figure 8), it is clear that the signal stabilizes after a short period of time.

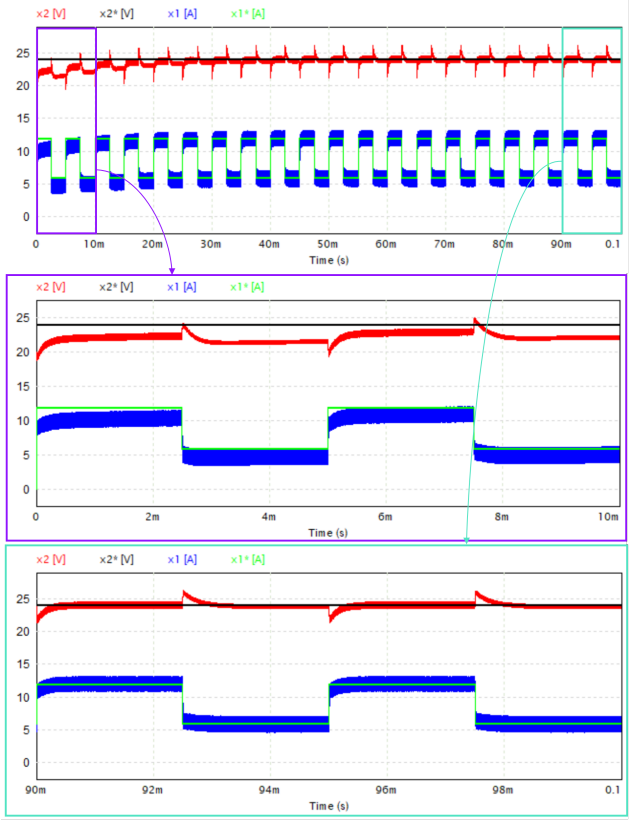

Figure 8: Boost converter dynamic response using the PI-PBC controller in the PSIM software

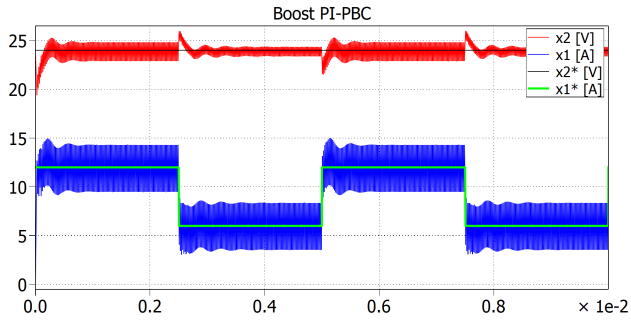

Figure 9: Simulation without the steady-state analysis tool

Figures 9 and 10 show the dynamic response of the PI-PBC implementation in PLECS. The simulation was run twice. In Figure 9, there is a clear perturbation in the dynamic response. To correct that, it was necessary to use the *steady-state analysis tool* (SSAT), which allows visualizing the signal when it enters a steady state. As shown in Figure 10,

the signal has an expected behavior that follows the reference signal with low error. In this case, before the SSAT is used, the simulation time is minimal; when the SSAT is used, it takes longer. This happens because the simulator has to evaluate the behavior many times until it finds the ”best” steady state signal.

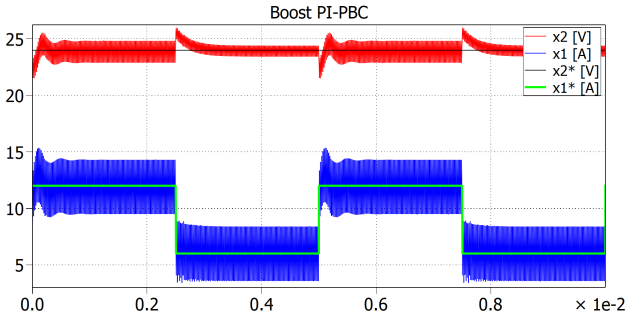

Figure 10: Simulation with the steady-state analysis tool

Figure 11 shows the dynamic response in MATLAB/Simulink. Even though the signal follows the reference, it does not behave as expected (*i.e.*, as shown in [11], [12], [29]). This is because the error is too high. It is possible to increase or decrease the tolerance in the simulation parameters, but the software takes too long to simulate, and the signal fails to reach the reference.

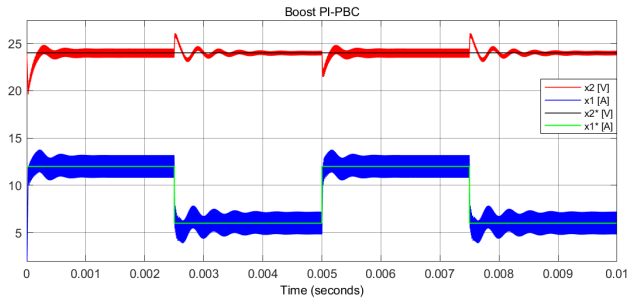

Figure 11: Boost converter dynamic response using PI-PBC controller in the MATLAB/Simulink software

4.2 IOC-PI Implementation

As well as the PI-PBC control law, the IOC-PI control law uses two positive proportional constants, as shown in Equation (21): also k_p and k_i with the same values.

Figure 12 shows the IOC-PI dynamic response of the implementation in PSIM. As with the PI-PB validation, the software takes some time to reach the reference. In comparison with the above-presented validation, the simulation time is shorter because this control technique uses a minimal number of elements [12].

Figures 13 and 14 show the dynamic response of the IOC-PI implementation in PLECS. As well as with the PI-PBC implementation, the SSAT had to be used. Without the SSAT, the signal does not reach the reference, and the error

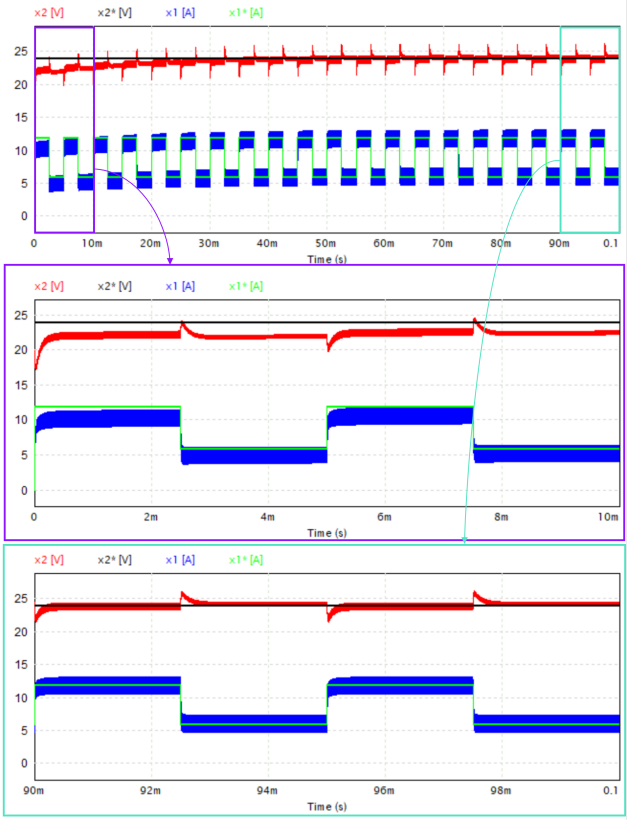

Figure 12: Boost converter dynamic response using IOC-PI controller in the PSIM software

is very high. When the SSAT is used, the signal reaches the reference and behaves as expected, minimizing the error.

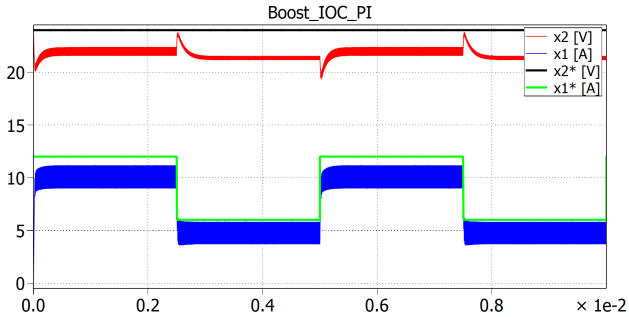

Figure 13: Simulation without the steady-state analysis tool in the PLECs software

In the case of MATLAB/Simulink, the dynamic response follows the reference signal with low accuracy, as is shown in Figure 15. In this case, even though the signal shows the expected behavior, the simulation time is very high when compared to the other software applications. This happens because, in order to get a response with high accuracy, the relative tolerance has to be set at a very low value (in this case, 1×10^{-7}).

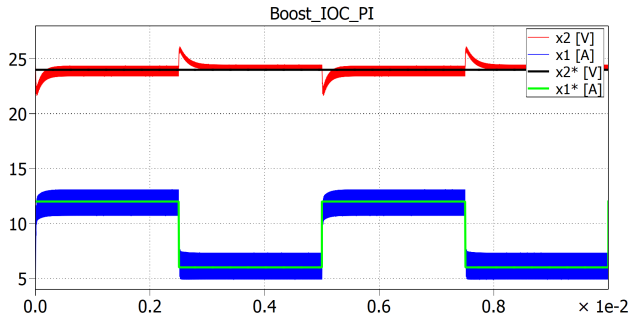

Figure 14: Simulation with the steady-state analysis tool in the PLECs software

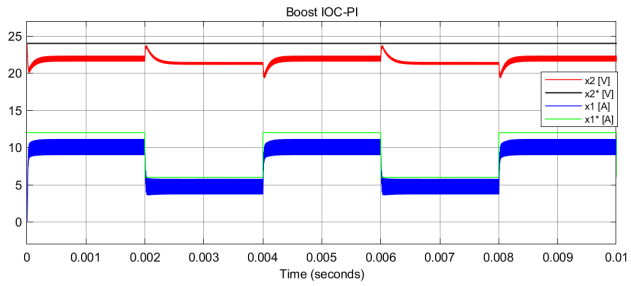

Figure 15: Boost converter dynamic response using the PI-PBC controller in the MATLAB/Simulink software

4.3 Discussion

To compare the studied software, the steady-state error (ε_{SS}) for the voltage signal (x_2) was obtained for each case. Table 2 shows the steady-state values, and Table 3 the steady-state error, obtained by comparison with the reference voltage signal x_2^*. The calculations for each software were made within an interval of $10ms$.

Table 2: Steady-state values of the voltage signal in each software application

SOFTWARE	STEADY-STATE VALUES [V]
PI-PBC	
PSIM	24.06665
PLECS (NO SSAT)	23.9207
PLECS (SSAT)	24.0247
MATLAB/SIMULINK	23.970
IOC-PI	
PSIM	24.39968
PLECS (NO SSAT)	21.7073
PLECS (SSAT)	24.078
MATLAB/SIMULINK	21.680

The software with the best performance in both controllers according to the steady-state error is PLECS (when the SSAT is used). The problem with it is that the simulation time is very high because it has to iterate many times until it finds the minimum error in accordance with a given tolerance value. MATLAB/Simulink has a good response in the PI-PBC validation, but a very poor performance in the IOC-PI validation, and it cannot be improved with a tool or technique, as is the case of PLECS. PSIM has a good performance, with very low errors in both cases.

Table 3: Steady-state error of the voltage signal in each software application

SOFTWARE	STEADY-STATE ERROR (ε_{SS} [%])
PI-PBC	
PSIM	0.27770833333333
PLECS (NO SSAT)	0.3304166667
PLECS (SSAT)	0.1029166667
MATLAB/SIMULINK	0.125
IOC-PI	
PSIM	1.665333333333334
PLECS (NO SSAT)	9.552916667
PLECS (SSAT)	0.325
MATLAB/SIMULINK	9.666666666667

5 Conclusions

In this study, the numerical validation of two types of nonlinear control (PI-PBC and IOC-PI) for the Boost converter was conducted in three different simulation software platforms, namely PSIM, PLECS, and MATLAB/Simulink. The dynamic response of the output voltage and the current flowing through the inductor was observed. Despite the fact that the three applications have their own strengths and weaknesses regarding simulation in power electronics and nonlinear control, the most accurate and easiest to use is PSIM. This one is highly recommended because it has a closer behavior to real applications. As explained in Section 4, PSIM uses direct measurements from the circuit itself; the other software must include techniques to obtain the necessary values on which the control law depends. Moreover, PSIM is recommended for users who have never used simulation software, as it is a more user-friendly environment, and it is easier to use and learn when compared to PLECS and MATLAB/Simulink. It is important to mention that there is a way to jointly use MATLAB/Simulink and PSIM or PLECS. The incorporation of two software environments can be useful if one is missing some features. Thus, the applications complement each other, allowing to perform more complex implementations.

Financial support: This paper did not have financial support.

Conflict of interest declaration: The authors declare no conflict of interest.

References

[1] J. P. J. Petinrin and M. S. M. Shaaban, "Overcoming challenges of renewable energy on future smart grid," *TELKOMNIKA (Telecommunication Computing Electronics and Control)*, vol. 10, no. 2, p. 229, 2012. DOI: 10.12928/telkomnika.v10i2.781.

[2] Erdiwansyah, Mahidin, H. Husin, Nasaruddin, M. Zaki, and Muhibbuddin, "A critical review of the integration of renewable energy sources with various technologies," Tech. Rep. 1, 2021. DOI: 10.1186/s41601-021-00181-3.

[3] H. Guldemir, "Sliding Mode Control of Dc-Dc Boost Converter," *Journal of Applied Sciences*, vol. 5, no. 3, pp. 588–592, 2005. DOI: 10.3923/jas.2005.588.592.

[4] R. E. Torres-Olguin, A. Garces, and G. Bergna, "HVDC transmission for offshore wind farms," in *Large Scale Renewable Power Generation*. Springer Singapore, 2014, pp. 289–310. DOI: 10.1007/978-981-4585-30-9_11.

[5] N. Mohan, *Electrónnica de potencia: convertidores, aplicaciones y diseño*. México: McGraw Hill, 2009, ISBN: 9789701072486.

[6] J.-K. Shiau and C.-W. Ma, "Li-ion battery charging with a buck-boost power converter for a solar powered battery management system," *Energies*, vol. 6, no. 3, pp. 1669–1699, 2013. DOI: 10.3390/en6031669.

[7] S. D. Mitchell, S. M. Ncube, T. G. Owen, and M. H. Rashid, "Applications and market analysis of DC-DC converters," in *2008 International Conference on Electrical and Computer Engineering*, IEEE, 2008. DOI: 10.1109/icece.2008.4769337.

[8] M. Namnabat, M. B. Poodeh, and S. Eshtehardiha, "Comparison the control methods in improvement the performance of the DC-DC converter," in *2007 7th Internatonal Conference on Power Electronics*, IEEE, 2007. DOI: 10.1109/icpe.2007.4692386.

[9] H. Li and X. Ye, "Sliding-mode PID control of DC-DC converter," in *2010 5th IEEE Conference on Industrial Electronics and Applications*, IEEE, 2010. DOI: 10.1109/iciea.2010.5516952.

[10] A. A. S. Khan and K. M. Rahman, "Voltage mode control of single phase boost inverter," 2008. DOI: 10.1109/icece.2008.4769293.

[11] W. Gil-González, O. D. Montoya, C. Restrepo, and J. C. Hernández, "Sensorless Adaptive Voltage Control for Classical DC-DC Converters Feeding Unknown Loads: A Generalized PI Passivity-Based Approach," *Sensors*, vol. 21, no. 19, p. 6367, 2021.

[12] J. S. Gómez-Chitiva, A. F. Escalante-Sarrias, and O. D. Montoya, "Voltage Regulation in Second-Order Dc-Dc Converters Via the Inverse Optimal Control Design with Proportional-Integral Action," *TecnoLógicas*, vol. 25, no. 55, e2369, 2022. DOI: 10.22430/22565337.2369.

[13] P. inc., *Psim user's guide version 2020a*, 2020. [Online]. Available: https://www.powersimtech.com/wp-content/uploads/2021/01/PSIM-User-Manual.pdf.

[14] P. GmbH, *Plecs user manual version 4.6*. [Online]. Available: https://www.plexim.com/files/plecsmanual.pdf.

[15] S. Documentation, *Simulation and model-based design*, 2020. [Online]. Available: https://www.mathworks.com/products/simulink.html.

[16] A. Devices, *Ltspice*. [Online]. Available: https://www.analog.com/en/design-center/design-tools-and-calculators/ltspice-simulator.html.

[17] S. Khader, A. Hadad, and A. A. Abu-aisheh, "The application of PSIM & matlab/simulink in power electronics courses," in *2011 IEEE Global Engineering Education Conference (EDUCON)*, IEEE, 2011. DOI: 10.1109/educon.2011.5773124.

[18] D. Baimel, R. Rabinovici, and S. Ben-Yakov, "Simulation of thyristor operated induction generator by simulink, psim and plecs," in *2008 18th International Conference on Electrical Machines*, IEEE, 2008.

[19] L. Allain, A. Merdassi, and L. Gerbaud, "Automatic modelling of Power Electronic Converter, Average model construction and Modelica model generation," in *Linkoping Electronic Conference Proceedings*, Linkoping University Electronic Press, 2009. DOI: 10.3384/ecp09430092.

[20] Q.-C. Zhong and M. Stefanello, "Port-hamiltonian control of power electronic converters to achieve passivity," in *2017 IEEE 56th Annual Conference on Decision and Control (CDC)*, IEEE, 2017. DOI: 10.1109/cdc.2017.8264413.

[21] R. Cisneros, M. Pirro, G. Bergna, R. Ortega, G. Ippoliti, and M. Molinas, "Global Tracking Passivity-based PI Control of Bilinear Systems and its Application to the Boost and Modular Multilevel Converters," *IFAC-PapersOnLine*, vol. 48, no. 11, pp. 420–425, 2015. DOI: 10.1016/j.ifacol.2015.09.222.

[22] G. Espinosa-Pérez, "Control de microrredes eléctricas de potencia: Un enfoque hamiltoniano," *Revista Iberoamericana de Automática e Informática industrial*, vol. 19, no. 4, pp. 442–451, 2022. DOI: 10.4995/riai.2022.17020.

[23] M. Zhang, P. Borja, R. Ortega, Z. Liu, and H. Su, "PID Passivity-Based Control of Port-Hamiltonian Systems," *IEEE Transactions on Automatic Control*, vol. 63, no. 4, pp. 1032–1044, 2018. DOI: 10.1109/tac.2017.2732283.

[24] A. Macchelli, "Passivity-based control of implicit port-hamiltonian systems," in *2013 European Control Conference (ECC)*, IEEE, 2013. DOI: 10.23919/ecc.2013.6669288.

[25] K. F. Krommydas and A. T. Alexandridis, "Design and passivity-based stability analysis of a PI current-mode controller for dc/dc boost converters," in *2014 American Control Conference*, IEEE, 2014. DOI: 10.1109/acc.2014.6859156.

[26] K. López-Rodríguez, W. Gil-González, and A. Escobar-Mejía, "Design and implementation of a PI-PBC to manage bidirectional power flow in the DAB of an SST," *Results in Engineering*, vol. 14, p. 100 437, 2022. DOI: 10.1016/j.rineng.2022.100437.

[27] F. M. Serra and C. H. D. Angelo, "IDA-PBC controller design for grid connected Front End Converters under non-ideal grid conditions," *Electric Power Systems Research*, vol. 142, pp. 12–19, 2017.

[28] H. Ramirez and Y. L. Gorrec, "An Overview on Irreversible Port-Hamiltonian Systems," *Entropy*, vol. 24, no. 10, p. 1478, 2022. DOI: 10.3390/e24101478.

[29] W. Gil-González, O. D. Montoya, and G. Espinosa-Perez, "Adaptive control for second-order DC–DC converters: PBC approach," in *Modeling, Operation, and Analysis of DC Grids*, Elsevier, 2021, pp. 289–310.

[30] C. Vega and R. Alzate, "Inverse optimal control on electric power conversion," in *2014 IEEE International Autumn Meeting on Power, Electronics and Computing (ROPEC)*, IEEE, 2014.